JOURNAL OF AGRICULTURAL AND FOOD CHEMISTRY
ARTICLE

J. Agric. Food Chem. 2010, 58, 6157–6165 6157
DOI:10.1021/jf100172e

Expression of Genes Associated with Aroma Formation Derived from the Fatty Acid Pathway during Peach Fruit Ripening

Bo Zhang,[†,‡] Ji-yuan Shen,[†] Wen-wen Wei,[†] Wan-peng Xi,[†] Chang-Jie Xu,[†] Ian Ferguson,[§] and Kunsong Chen*[,†]

[†]Laboratory of Fruit Quality Biology, Huajiachi Campus, Zhejiang University, Hangzhou 310029, China, [‡]The State Agriculture Ministry Laboratory of Horticultural Plant Growth, Development and Quality Improvement, Hangzhou 310029, China, and [§]The New Zealand Institute of Plant and Food Research, Mt. Albert Research Centre, Auckland 1025, New Zealand

Changes in characteristic aroma volatiles, levels of fatty acids as aroma precursors, and expression patterns of related genes, including lipoxygenase (LOX), hydroperoxide lyase (HPL), alcohol dehydrogenase (ADH), alcohol acyltransferase (AAT), and fatty acid desaturase (FAD), were studied in peach (*Prunus persica* L. Batsch., cv. Yulu) fruit during postharvest ripening at 20 °C. Concentrations of *n*-hexanal, (*E*)-2-hexenal, (*E*)-2-hexenol, and (*Z*)-3-hexenol decreased, whereas the production of (*Z*)-3-hexenyl acetate, γ-hexalactone, γ-octalactone, γ-decalactone, and δ-decalactone increased with fruit ripening. Lactones showed a clear pattern concomitant with the climacteric rise in ethylene production, with γ-decalactone being the principal volatile compound at the late ripening stage. Of the LOX family genes, *PpLOX2* and *PpLOX3* had relatively high transcript levels initially followed by a decline with fruit ripening, while levels of *PpLOX1* and *PpLOX4* transcripts were upregulated by accumulated ethylene production. Expression of *PpHPL1*, *PpADH1*, *PpADH2*, and *PpADH3* showed similar decreasing patterns during ripening. Expression levels of *PpAAT1* showed a rapid increase during the first 2 days of postharvest ripening followed by a gradual decrease. Contents of polyunsaturated linoleic and linolenic acids increased, and saturated palmitic acid levels tended to decline as the fruit ripened. The increased levels of unsaturated fatty acids closely paralleled increasing expression of *PpFAD1* and *PpFAD2*. The significance of gene expression changes in relation to aroma volatile production is discussed.

KEYWORDS: Alcohol acyltransferase; alcohol dehydrogenase; aroma volatiles; fatty acid; fatty acid desaturase; hydroperoxide lyase; lipoxygenase; peach

INTRODUCTION

Peach fruit aroma volatiles have been intensively studied in the past, and more than 100 compounds have been identified (*1*, *2*). Among the large number of volatiles present in peach fruit, only a few are considered as impact aroma compounds. These include lactones, mainly γ- and δ-decalactones, and C6 aldehydes and alcohols, such as *n*-hexanal, (*E*)-2-hexenal, and (*E*)-2-hexenol (*3*, *4*). In addition, esters, such as (*Z*)-3-hexenyl acetate, contribute to peach fruit aroma (*4*). The lactones and esters provide fruity notes, and the C6 compounds contribute green sensory notes in the ripening fruit.

Six carbon aldehydes and alcohols are biosynthesized from linoleic and linolenic acids through a sequence of enzyme reactions known as the lipoxygenase (LOX) pathway (*5*). First, LOX produces hydroperoxide isomers of both linoleic and linolenic acids, which are subsequently cleaved by hydroperoxide lyase (HPL) to form hexanal and hexenal, respectively. The aldehydes can then be reduced to the corresponding C6 alcohols by alcohol dehydrogenase (ADH). Alcohol acyltransferase (AAT) catalyzes the final linkage of an acyl moiety and an alcohol to form esters and, thus, are directly responsible for the production of esters. Lactones are another major group of fatty-acid-derived volatile compounds; however, specific enzymes and genes involved in this pathway have not been characterized (*5*). As mentioned above, peach characteristic aroma volatile compounds are mainly generated through the fatty acid pathway.

Volatile production from the fatty acid pathway in other fruit, such as tomato, has been studied using transgenic approaches to up- or downregulate genes with the aim of improving fruit aroma quality (*6*). A mutation in fatty acid desaturase (FAD) has been shown to result in the deficiency of linolenic acid in a *Lefad7* mutant tomato and reduce hexenals and hexenols derived from linolenic acid (*7*). The overexpression of a yeast FAD gene in tomato caused changes in the fatty acid profile and altered levels of C6 volatile compounds (*8*, *9*). Moreover, transgenic approaches have been used to determine the relative importance of LOX (*10*), HPL (*11*), and ADH (*12*) in the generation of C6

*To whom correspondence should be addressed. Telephone: +86-571-86971931. Fax: +86-571-86971630. E-mail: akun@zju.edu.cn.

Published on Web 04/23/2010

aldehydes and alcohols in tomato fruit. Progress in the identification of genes and enzymes responsible for fruit volatile formation has been reviewed by Defilippi et al. (*13*). Apart from tomato fruit, LOX gene family members involved in aroma volatile biosynthesis have been studied in apple (*14*), kiwifruit (*15*), and olive (*16*), HPL gene family members involved in aroma volatile biosynthesis have been studied in guava fruit (*17*) and melon (*18*), ADH gene family members involved in aroma volatile biosynthesis have been studied in melon (*19*) and apricot fruit (*20*), and AAT gene family members involved in aroma volatile biosynthesis have been studied in apple (*21*), melon (*22*), and strawberry fruit (*23*).

Most previous studies have reported that the specific peach fruit volatiles are dependent upon the cultivar (*2*, *3*), fruit maturity (*4*, *24*−*26*), and postharvest storage conditions (*27*−*30*). A possible involvement of LOX, ADH, and fatty acids in the biosynthesis of peach fruit aromas has been proposed (*31*, *32*). However, changes in volatiles during postharvest ripening and the relationship with expression of genes involved in the fatty acid pathway, to our knowledge, have not been studied. In the present work, postharvest changes in characteristic peach fruit aroma volatiles and their precursor fatty acids were analyzed. Four FAD, four LOX, one HPL, three ADH, and one AAT gene from the fatty acid pathway were cloned from peach flesh tissue, and their expression profiles were estimated during postharvest ripening using real-time quantitative polymerase chain reaction (PCR). The possible roles played by ethylene and the gene family member in the development of characteristic aroma volatiles of peach fruit are discussed.

MATERIALS AND METHODS

Chemicals and Reagents. The reference compounds used for volatile studies were supplied by Fluka, except for 2-octanol, which was purchased from Sigma-Aldrich. Chemical standards used for fatty acid identification were obtained from Sigma-Aldrich. Other chemicals were of analyzed grade and supplied by Shanghai Sangon Engineering and Biotechnology Services Company Limited.

Plant Material and Tissue Sampling. Melting flesh peach (*Prunus persica* L. Batsch cv. Yulu) fruit were harvested at commercial maturity from Ningbo, Zhejiang Province, China. In our experiment, harvest was based on color, which was measured using MiniScan XE plus (Hunter Associates Laboratory, Inc., Reston, VA). Lightness (L) was measured directly, and hue angle (H_{ab}) and chroma (C^*) were calculated (*33*). Fruit with $L = 68.76 \pm 1.95$, $H_{ab} = 78.81 \pm 1.87$, and $C^* = 25.15 \pm 1.17$ were selected. Fruit were transported to the laboratory on the day of harvest and screened for uniform size and freedom from visible defects or decay. The fruit were stored at 20 °C for 7 days to allow for postharvest ripening and sampled every day. At each sampling time, slices of mesocarp (about 1 cm thick) were combined and frozen in liquid nitrogen and stored at −80 °C for further use. For biochemical and molecular analyses, three replicates of three fruit each were used.

Fruit Ripening Evaluations. Fruit were placed in three 2 L flasks, 3 fruit per flask, and capped with a rubber stopper for 1 h. Ethylene was measured according to Zhang et al. (*15*). A total of 1 mL of headspace gas from each flask was sampled using a syringe and then was analyzed using gas chromatography (GC, SP 6800, Lu'nan Chemical Engineering Instrument, Shandong, China) fitted with a GDX-502 column. Nitrogen was used as a carrier gas at 20 mL min^{-1}. The injector, detector, and oven temperatures were 110, 140, and 90 °C, respectively.

Fruit firmness was measured at the equator of the fruit using a TA-XT2i Plus texture analyzer (Stable Micro System, U.K.) fitted with a 7.9 mm diameter head. The rate of penetration was 1 mm s^{-1}, with a final penetration depth of 10 mm, and data are expressed in newtons. Two measurements were made on opposite sides of each fruit after the removal of a 1 mm thick slice of skin.

Total soluble solids (TSS) were measured by slicing both ends of each of the same 9 fruit, and three drops of juice from each slice were then applied to an Atago PR-101α digital hand-held refractometer.

Four flesh cubes (about 1 cm^3) were taken from opposite sides of each fruit and used for juiciness analysis using a texture analyzer (TA-XT2i Plus) with a 10 cm diameter head. The rate of penetration was 0.5 mm s^{-1} with a force of 100 N held for 8 s. The weight of juice released by the pressure produced from the texture analyzer was determined, and the crushed flesh remaining was also weighed. The proportion of juice in relation to the total flesh (mass/mass) was calculated and expressed as a percentage, a method previously described by Infante et al. (*34*).

Volatile Analysis. Measurement of volatiles was carried out according to Zhang et al. (*15*), with modifications. A total of 5 g of frozen flesh tissue was ground in liquid nitrogen and transferred to a 15 mL vial containing 5 mL of saturated sodium chloride solution. Before the vials were sealed, 30 μL of 2-octanol (8.69 mg mL^{-1}) was added as an internal standard and stirred for 10 s with a vortex. For manual solid-phase microextraction (SPME) analysis, samples were equilibrated at 40 °C for 30 min and then exposed to a fiber coated with 65 μm of polydimethylsiloxane and divinybenzene (Supelco Co., Bellefonte, PA). The volatiles were subsequently desorbed over 5 min at 230 °C into the splitless injection port of the GC−flame ionization detector (FID). An Agilent 6890N GC equipped with a FID and a DB-WAX column (0.32 mm, 30 m, 0.25 μm, J&W Scientific, Folsom, CA) was used for volatile analysis. Chromatography conditions were as follows: injector, 230 °C; initial oven temperature, 34 °C held for 2 min, increased by 2 °C min^{-1} to 60 °C, then increased by 5 °C min^{-1} to 220 °C, and held for 2 min. Nitrogen was used as a carrier gas at 1.0 mL min^{-1}. Volatiles were identified by a comparison of retention times to those of authentic standards. To further identify volatile compounds produced from peach fruit, capillary gas chromatography−mass spectrometry (GC−MS) (6890N-5795B) analyses were performed using a HP-5MS column (0.25 mm, 30 m, 0.25 μm, J&W Scientific, Folsom, CA). Injection port temperature was 240 °C, with a split ratio of 5:1. Helium was used as the carrier gas at a rate of 1.0 mL min^{-1}. The column temperature was held at 40 °C for 2 min, increased by 5 °C min^{-1} to 60 °C, then increased by 10 °C min^{-1} to 250 °C, and held for 5 min. MS conditions were as follows: ion source, 230 °C; electron energy, 70 eV; multiplier voltage, 1247 V; GC−MS interface zone, 280 °C; and a scan range, 30−250 mass units. Volatiles were identified on the basis of a comparison of their electron ionization (EI) mass spectra to published data and data from authentic standards. Quantitative determination of compounds was carried out using the peak of the internal standard as a reference value and calculated on the basis of standard curves of authentic compounds.

Fatty Acid Analysis. The total fatty acid profile was determined according to Zhang et al. (*15*). Briefly, 6 g of frozen powdered fruit tissue was used to extract total lipids by gentle shaking in a mixture of chloroform/methanol/water (1:2:0.8, v/v/v) at room temperature. After centrifugation at 5000 *g* for 15 min at 4 °C, the upper phase was extracted with 8 mL of chloroform and NaCl (0.76%, w/v) and the organic phase was dried under a nitrogen stream. The residue was dissolved in 2 mL of hexane and stored at −20 °C for further analysis. Total fatty acids were transformed into their corresponding fatty acid methyl ester (FAME) by the addition of 2 mL of H_2SO_4 (2.5% in methanol, v/v), and a known amount of heptadecanoic acid (C17:0) was added as an internal standard. A GC−FID (Agilent 6890N) equipped with a DB-23 column (0.25 mm, 60 m, 0.25 μm, J&W Scientific, Folsom, CA) was used for fatty acid analysis. Helium at 1.2 mL min^{-1} was used as the carrier gas. Conditions for chromatography were as follows: injection, 250 °C; initial oven temperature, 50 °C, increased to 175 °C at 25 °C min^{-1}, increased to 230 °C at 4 °C min^{-1}, and held for 5 min. Identification of compounds was confirmed by comparisons to authenticated reference standards. Quantitative determination of compounds was carried out using the peak of the internal standard as a reference value and calculated on the basis of the standard curve of authentic compounds.

RNA Extraction and cDNA Synthesis. Total RNA was isolated from approximately 3 g of frozen tissues following the protocol described by Zhang et al. (*35*). Contaminating genomic DNA was removed by RNase-free DNase I (Fermentas) treatment. The concentration of isolated total RNA was determined by the absorbance at 260 nm (A_{260}) using a NanoDrop ND-3300 fluorospectrometer with Quant-iT RiboGreen RNA reagent (Invitrogen) following the instructions of the manufacturer, and the integrity was evaluated by electrophoresis on 1.0% agarose gels. The cDNA was synthesized from 3.0 μg of DNA-free RNA with RevertAid

Table 1. Primers for Real-Time qPCR Analysis

gene	GenBank accession number	forward primer (5′−3′)	reverse primer (5′−3′)	product size (bp)
PpLOX1	EU883638	GGCAATTAGGAAAAGTGGTTG	TGCGCAATATTTTTGGTGTG	65
PpLOX2	FJ029110	GTGGACTCACTGGGAGAGGA	GTTGCACGACCATTTCACAC	125
PpLOX3	FJ032015	CATCCTTCTAGTGAGGCTGGA	GGAGAAGCATTAAATTGAGACACTG	69
PpLOX4	EF568783	TCCTTCTCTCTTGGCTCGAT	GGGCTTGCATTCGCATAGTA	95
PpHPL1	DW354957	AAATGGGGATGTGATGGATG	TTGCCCTTTTCCCTCAAGTA	115
PpADH1	DY648995	AACGCCCGACTAGTTTGTTG	CGATCATTCTTCGGCAAATC	61
PpADH2	DY641017	GATTTGATGCTTTCAGGACAGT	CCAAGTTGCTCTAATCCTCCA	138
PpADH3	DY636352	TGACATGGAAACTATGAACAGC	TTGAATGGAGGCTGATGGTT	109
PpAAT1	DY645545	TTGGAGAGGTTTGAGGAGGA	AGCCCACACAACACAAGACA	111
PpFAD1	AJ824111	CGGTTTTCAAGGCAATGTTC	CCTACACTCATTCGGGCAAT	135
PpFAD2	AJ822450	AGTGACCCAGGAGATATTGTGT	TTCGAAAGATTACGAGGATTTCA	87
PpFAD3	AJ873289	TCAGGCACAACAATTGAAGC	AAGAATGGCTGCCCATACAG	113
PpFAD4	AJ876286	ACGTTGCCTTTGACCAACTT	AATGACTGTGACCCCACCAC	116

Premium reverse transcriptase (Fermentas) and oligo $d(T)_{18}$ as primers followed the protocol of the manufacturer. The first strand cDNA was diluted for real-time quantitative PCR (qPCR) analysis. For each time point, three batches of RNA were isolated for separate cDNA synthesis.

Gene Isolation and Oligonucleotide Primers. The ESTree database (http://www.itb.cnr.it/estree/index.php) represents a collection of *P. persica* expressed sequence tags (ESTs) and is intended as a resource for peach functional genomics (*36*). ESTs were downloaded on March 16th, 2009 and analyzed using SeqMan II (version 5.01, Demonstration System, DNASTAR, Inc., Madison, WI). The 3′-untranslated regions (UTRs) of candidate sequences were amplified using SMART RACE cDNA amplification kit (Clontech). On the basis of the present sequence information, there are likely to be at least four FAD genes, four LOX genes, one HPL gene, three ADH genes, and one AAT gene in peach fruit flesh tissue. Alignment for the phylogenetic analysis was calculated with ClustalW1.82 (http://ibi.zju.edu.cn/clustalw/). The phylogenetic tree was drawn using Tree-View with default parameters (http://www.bioon.com/Soft/Class1/Class13/200408/127.html).

The oligonucleotide primers for real-time qPCR analysis were designed on the basis of the 3′-UTR of individual genes, using Primer3 online (version 0.4.0, http://frodo.wi.mit.edu/primer3/input.htm). The size of all PCR products ranged from 60 to 150 bp. Primer specificity and quality tests for primers were performed according to Zhang et al. (*35*). The sequences of all primers used for qPCR are described in **Table 1**.

Real-Time qPCR Analysis. The qPCR reactions were performed in a total volume of 20 μL, 200 μM for each primer, 10 μL of 2 × SYBR Premix Ex Taq PCR Master Mix (TaKaRa), and 1.0 μL of the diluted cDNA in LightCycler 1.5 real-time PCR instrument (Roche). The temperature program included a preliminary step of 30 s at 95 °C, followed by 40 cycles of 94 °C × 5 s and 60 °C × 20 s. No template controls for each primer pair were included in each run. Peach *TEF2* (TC3544) was used as an internal control to normalize small differences in template amounts according to Tong et al. (*37*). At least three different RNA isolations and cDNA syntheses were used as replicates for the qPCR. Expression levels produced by the qPCR were expressed as a ratio relative to the fruit at the harvest time point, which was set to 1.

Experimental Design and Statistical Analysis. A completely randomized design was used in the experiments. Standard errors (SEs) and figures were made by OriginPro 7.5 G (Microcal Software, Inc., Northampton, MA). Differences indicated in the figures were based on a least significant difference (LSD) test at the 5% level (DPS version 2.00, Zhejiang University, China). To provide a general overview of the relationship between volatile production and gene expression, a principal component analysis (PCA) was developed using AlphaSoft version 11.0 (Alpha MOS, Toulouse, France). Samples were characterized by volatile emissions and gene expression according to Zhang et al. (*38*). Data were centered and weighted using the data reduction algorithm to avoid dependence upon measured units and to reduce the weight of large peaks, so that the minor peaks have the same impact. This methodology ensures that the weighting on variables in the PCA is not unit-dependent, otherwise larger valued units that vary more will be dominant in the PCA.

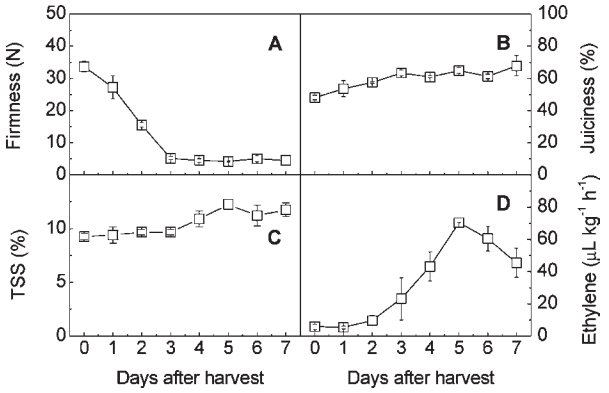

Figure 1. (A) Fruit firmness, (B) juiciness, (C) TSS, and (D) ethylene production of peach fruit during postharvest ripening at 20 °C.

RESULTS

Peach Fruit Firmness, Juiciness, TSS, and Ethylene Production during Postharvest Ripening. As expected, fruit firmness decreased rapidly from 33.64 N at harvest to 5.17 N after 3 days of ripening at 20 °C and then remained at a constant level (**Figure 1A**). Loss of firmness was concomitant with changes in juiciness that increased rapidly at about 3 days (**Figure 1B**) and with accumulation of TSS with fruit ripening (**Figure 1C**). The climacteric rise in ethylene production of fruit held at 20 °C was initiated at about 3 days after harvest, reaching a peak of about 70.38 μL kg^{-1} h^{-1} on the 5th day of ripening, and then declined (**Figure 1D**).

Volatile Compound Production during Fruit Ripening. The green aroma of peach fruit comprises C6 volatile compounds, such as *n*-hexanal, (*E*)-2-hexenal, *n*-hexanol, (*E*)-2-hexenol, and (*Z*)-3-hexenol. Peach fruit *n*-hexanal showed the highest concentrations, followed by (*E*)-2-hexenal and C6 alcohols. There was a rapid decline in the content of *n*-hexanal and (*E*)-2-hexenal during the first day of postharvest fruit ripening, with the loss being in the order of 50% (panels **A** and **B** of **Figure 2**). The concentrations of (*E*)-2-hexenol and (*Z*)-3-hexenol were high at harvest, significantly decreased after 1 day of ripening, then were maintained for 2 days followed by a significant decline again during fruit ripening (panels **C** and **D** of **Figure 2**). Ester (*Z*)-3-henenyl acetate showed low levels during the first 4 days of ripening and then exhibited a sharp increase up to 7 days at 20 °C (**Figure 2E**).

The fruity aroma of peach is mainly composed of lactonic compounds. Levels of γ-hexalactone, γ-decalactone, and δ-decalactone were low or under detection limits on the initial day and increased rapidly along with the climacteric rise of ethylene during fruit ripening (panels **F**, **H**, and **I** of **Figure 2**). The volatile γ-octalactone was found at medium levels at harvest,

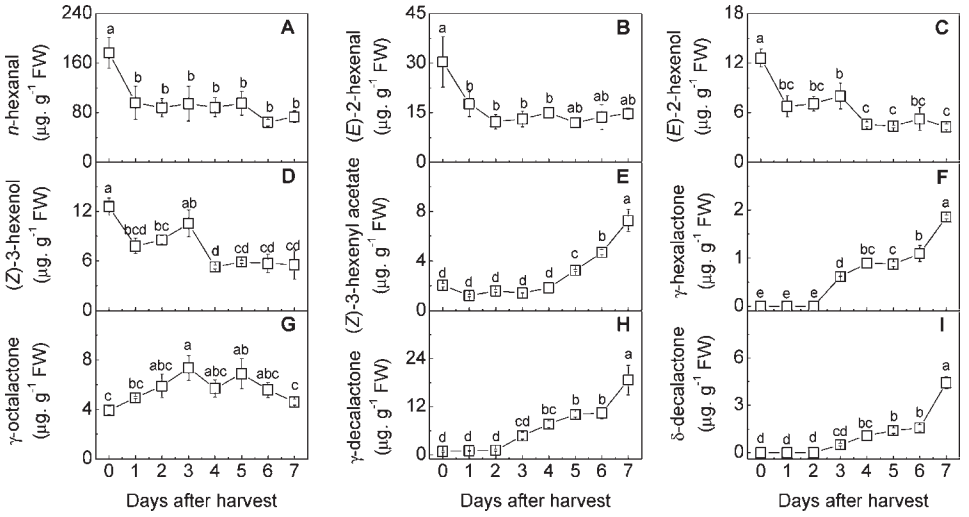

Figure 2. Production of (A) *n*-hexanal, (B) (*E*)-2-hexenal, (C) (*E*)-2-hexenol, (D) (*Z*)-3-hexenol, (E) (*Z*)-3-hexenyl acetate, (F) γ-hexalactone, (G) γ-octalactone, (H) γ-decalactone, and (I) δ-decalactone during postharvest peach fruit ripening at 20 °C. Fruit aroma compounds were determined from headspace analysis by SPME and GC. Error bars indicate SE from three replicates. Values with different letters for LOX activity are different at $p < 0.05$.

accumulated during the first 3 days of ripening, and remained high until the end of the experimental period (**Figure 2G**). The major lactone identified on the day of harvest was γ-octalactone and was replaced by γ-decalactone in fully ripe fruit after 7 days.

Gene Cloning and Sequence Analysis. From the peach EST database and National Center for Biotechnology Information (NCBI), at least four expressed gene sequences were putative members of the LOX gene family. The four sequences were designated as *PpLOX1*−*PpLOX4* (Genbank accession numbers: EU883638, FJ029110, FJ032015, and EF568783, respectively). Phylogenetic analysis of translated amino acid sequences from different members of the known plant LOX families generated clusters that could be structured into the two main groups: 9-LOX and 13-LOX (**Figure 3A**). *PpLOX2*, *PpLOX3*, and *PpLOX4*, were clustered in the 9-LOX class together with the tomato LOX genes *TomLOXA* and *TomLOXB* and the potato gene *PotLX3*. The second group, 13-LOX, contains one member *PpLOX1*, together with the tomato genes *TomLOXC* and *TomLOXD* and kiwifruit genes *AdLOX2* and *AdLOX5*.

Similar to the LOX family, plant HPL genes was clustered into two groups based on deduced amino acid sequences (**Figure 3B**). One group consisted of two HPL genes from cucumber, *CsHPL1* and *CmHPL1*, which have been proposed to have fatty acid 9-HPL activity. Peach *PpHPL1* (DW354957) was located in another group (13-HPL) and clustered with *Arabidopsis AtHPL1*, guava fruit *PpHPL1*, tomato *LeHPL1*, and potato *StHPL1*. The highest identity was with 13-HPL from guava fruit *PpHPL1*.

According to the alignment of deduced amino acids, basically two groups of the ADH gene family were identified (**Figure 3C**). Three peach ADH genes, *PpADH1* (DY648995), *PpADH2* (DY641017), and *PpADH3* (DY636352) were grouped into one cluster, sharing 44−58, 62−84, and 62−74% homology with other plant ADH members in this group, respectively. The second group was composed of cucumber *CmADH2*, citrus *CsADH1*, and apricot *PaADH1*. The percentage of identity at the amino acid level between three peach ADH genes and the second group is quite low, ranging from 7 to 11%.

The phylogenetic tree of the AAT family shows three groups according to deduced amino acid sequences (**Figure 3D**). The first group comprises the two strawberry AATs, *FaAAT1* and *FvAAT1*. Cucumber *CmAAT4* is the only member of the second group. The third group is composed of three AATs from cucumber (*CmAAT1*, *CmAAT2*, and *CmAAT3*), two AATs from apple (*MdAAT1* and *MdAAT2*), apricot *PaAAT1*, and peach *PpAAT1* (DY645545). It is notable that AATs from *Prunus* species were located in one group. The deduced amino acid sequence of peach *PpAAT1* was approximately 86% identical to AAT from apricot.

Expression of LOX, HPL, ADH, and AAT Genes during Fruit Ripening. During postharvest ripening at 20 °C, *PpLOX1* and *PpLOX4* exhibited similar increasing expression patterns according to the relative qPCR results (**Figure 4**). In contrast, *PpLOX2* and *PpLOX3* had relatively higher transcript levels at harvest and then declined as the fruit ripened. There was a decline in *PpLOX2* levels immediately after harvest, and these remained low after 3 days. Expression levels of *PpLOX3* remained constant during the first 2 days, followed by a decline until the last day of the experiment. Overall, there were no large differences in abundance among the four LOX genes.

Expression of *PpHPL1* was at relatively high levels on the initial day and decreased progressively with ripening from 1 day onward, with a rapid decline 3 days after harvest (**Figure 4**).

The three members of the ADH gene family showed similar decreasing expression patterns with ripening, with relatively higher abundance 2 days after harvest and then lower but constant expression until day 7 (**Figure 4**).

Transcript levels of *PpAAT1* increased rapidly during the first 2 days of postharvest ripening at 20 °C, reaching maximal levels at about 2 days, followed by a gradual decrease up to 7 days of ripening (**Figure 4**).

Fatty Acid Contents in Ripening Fruit. We analyzed the levels of all major fatty acids to compare changes in specific substrates with general patterns of fatty acid contents during fruit ripening. The major fatty acid component in peach fruit at harvest (percentages give the range of contents) was palmitic acid (44−62%), followed by linoleic acid (29−34%), linolenic acid (6−8%), stearic acid (4−6%), and oleic acid (1−3%) (**Figure 5**). As the main substrates for LOX-catalyzed oxidation, polyunsaturated linoleic and linolenic acids showed accumulating profiles as the fruit ripened (panels **D** and **E** of **Figure 5**). Concentrations of linoleic acid increased over 6 days and then declined during ripening at 20 °C. Linolenic acid tended to accumulate through the ripening period, with an increase of 110% after 7 days. The major saturated fatty acid, palmitic acid, showed a 2-fold

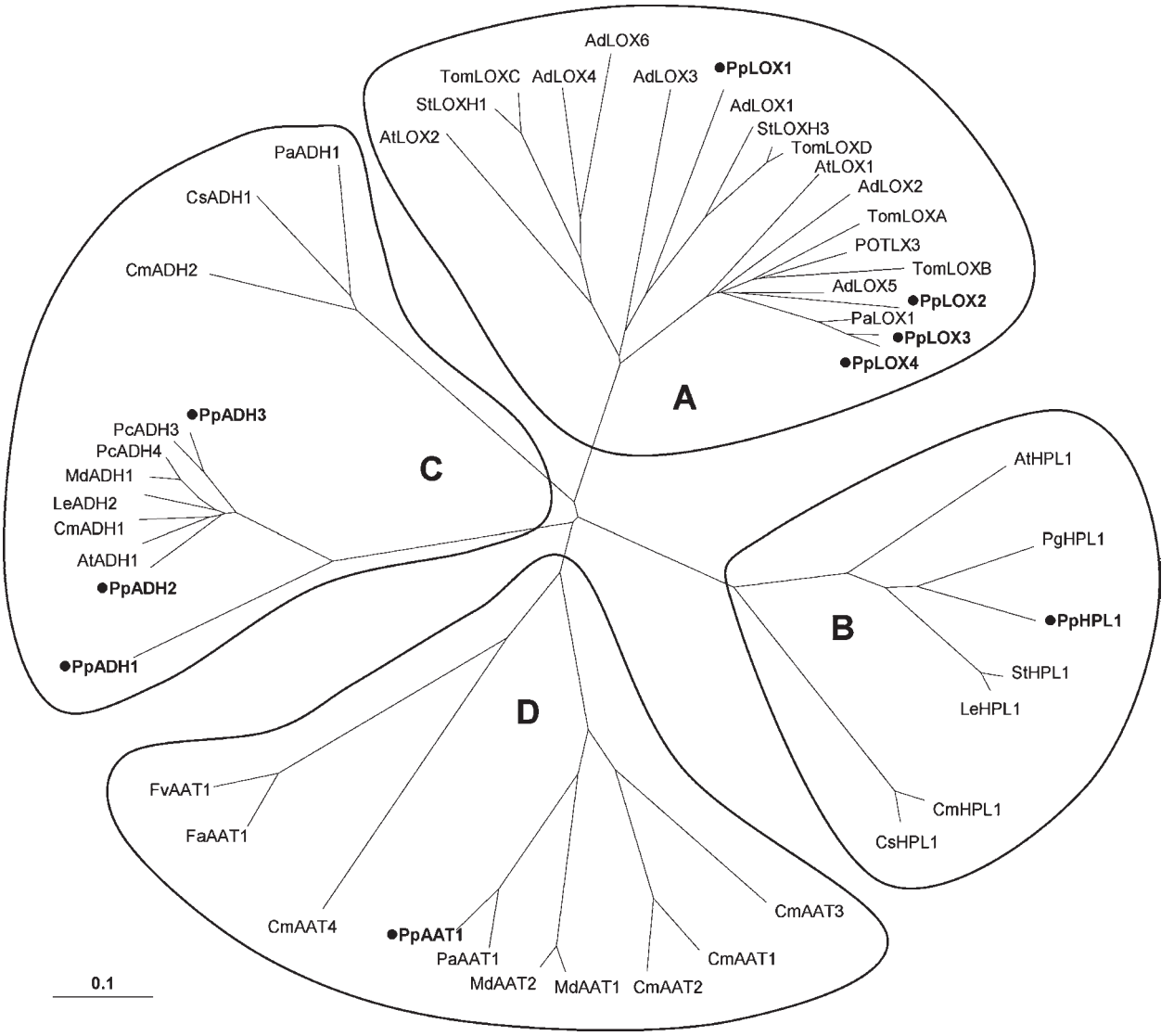

Figure 3. Phylogenetic analysis of (A) LOX, (B) HPL, (C) ADH, and (D) AAT from peach and other plants. Data were organized using ClustalW and TreeView software with default parameters. Peach sequences are indicated in bold. Accession numbers of sequences used to build the tree: *AdLOX1* (DQ497792), *AdLOX2* (DQ497797), *AdLOX3* (DQ497795), *AdLOX4* (DQ497793), *AdLOX5* (DQ497796), *AdLOX6* (DQ497794), *AtLOX1* (AAA32827), *AtLOX2* (AAA32749), *TomLOXA* (AAA53184), *TomLOXB* (AAA53183), *TomLOXC* (AAB65766), *TomLOXD* (AAB65767), *POTLX3* (AAB67865), *StLOXH1* (CAA65268), *StLOXH3* (CAA65269), *PpLOX1* (EU883638), *PpLOX2* (FJ029110), *PpLOX3* (FJ032015), *PpLOX4* (EF568783), *AtHPL1* (AAC69871), *PgHPL1* (AAK15070), *PpHPL1* (DW354957), *StHPL1* (CAC44040), *LeHPL1* (AAF67142), *CmHPL1* (AAK54282), *CsHPL1* (AAF64041), *AtADH1* (AAK73970), *CmADH1* (ABC02081), *CmADH2* (ABC02082), *CsADH1* (CX049468), *LeADH2* (CAA54450), *MdADH1* (CAA88271), *PaADH1* (ABZ79222), *PcADH3* (AAB86868), *PcADH4* (AAB86869), *PpADH1* (DY648995), *PpADH2* (DY641017), *PpADH3* (DY636352), *CmAAT1* (CAA94432), *CmAAT2* (AAL77060), *CmAAT3* (AAW51125), *CmAAT4* (AAW51126), *MdAAT1* (AY707098), *MdAAT2* (AY517491), *FaAAT1* (AAG13130), *FvAAT1* (AAN07090), *PaAAT1* (ACF07921), and *PpAAT1* (DY645545).

decrease over the 7 days of ripening (**Figure 5A**). Concentrations of other fatty acids, such as stearic and oleic acid, were relatively unchanged in the fruit ripening process (panels **B** and **C** of **Figure 5**).

Expression of the FAD Gene Family during Fruit Ripening. The transcript abundance of *PpFAD1* increased and peaked at about 4 days after harvest (**Figure 6**). *PpFAD2* remained at a relatively constant low level for 2 days and then increased concomitantly with the increase in the production of ethylene and linolenic acid at about 3 days during ripening. Expression patterns of *PpFAD3* and *PpFAD4* were similar, with transient increases 1 day after harvest, followed by constant expression levels.

Full-Data PCA Model during Fruit Ripening. PCA was performed to provide an overview of the complete data set in a reduced dimension plot. As shown in **Figure 7**, principal component 1 (PC1) and principal component 2 (PC2) accounted for about 78% of the total variability when ethylene, volatile compounds, and gene expression were used to characterize peach fruit ripening at 20 °C up to 7 days. In cluster A, samples at harvest (0 day) were characterized by C6 aldehydes, C6 alcohols, *PpLOX2*, *PpLOX3*, *PpHPL1*, *PpADH1*, *PpADH2*, and *PpADH3* and were separated from other samples during peach fruit ripening, indicating that these volatiles and genes were predominant in unripe fruit. Cluster B consisted of samples at 1, 2, and 3 days after harvest. Cluster C consisted of fruit at 4, 5, 6, and 7 days after harvest, characterized by ethylene, volatiles such as esters and lactones, polyunsaturated fatty acids, *PpLOX1*, *PpLOX4*, *PpFAD1*, and *PpFAD2*. PCA showed that downregulated genes

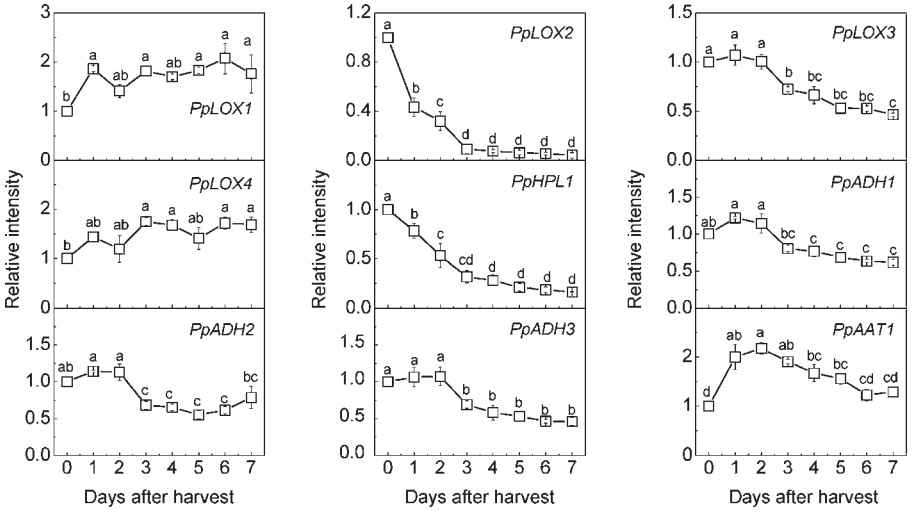

Figure 4. Expression of (A) LOX, (B) HPL, (C) ADH, and (D) AAT family transcripts in ripening peach fruit by real-time qPCR analysis. Error bars indicate SE from three replicates. Expression levels of each gene are expressed as a ratio relative to the harvest time (0 day), which was set at 1. Values with different letters for LOX activity are different at $p < 0.05$.

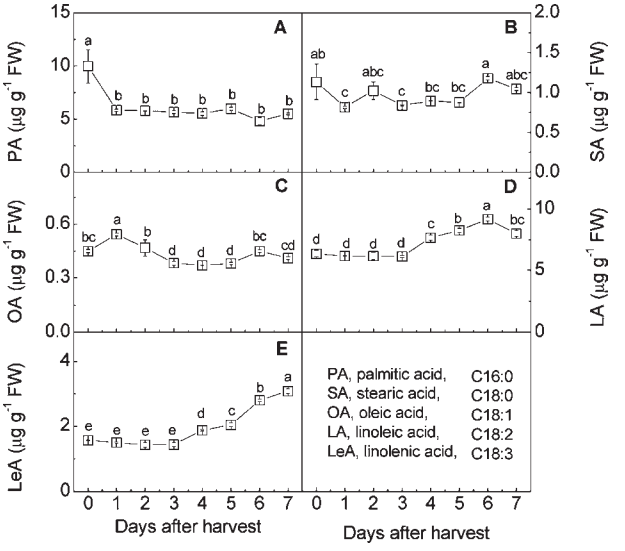

Figure 5. Changes in (A) palmitic, (B) stearic, (C) oleic, (D) linoleic, and (E) linolenic acids during peach fruit ripening at 20 °C. Error bars indicate SE from three replicates. Values with different letters for LOX activity are different at $p < 0.05$.

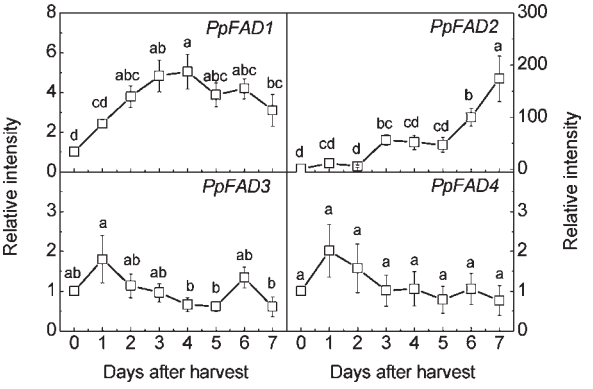

Figure 6. Expression of FAD gene family transcripts in ripening peach fruit by real-time qPCR analysis. Error bars indicate SE from three replicates. Expression levels of each gene are expressed as a ratio relative to the harvest time (0 day), which was set at 1. Values with different letters for LOX activity are different at $p < 0.05$.

and C6 volatiles were grouped and upregulated genes were clustered with accumulated esters and lactones associated with peach fruit ripening and senescence.

DISCUSSION

The characteristic aroma volatiles of ripening peach fruit fall into two groups. Concentrations of so-called green-note volatiles, *n*-hexanal, (*E*)-2-hexenal, (*E*)-2-hexenol, and (*Z*)-3-hexenol, were decreased with ethylene-dependent ripening. On the other hand, the fruity aroma volatiles, γ-hexalactone, γ-octalactone, γ-decalactone, and δ-decalactone, increased as ripening progressed. Previous studies suggested that C6 aldehydes and alcohols tended to decrease with peach fruit maturation and lactonic compounds accumulate in fruit of relatively higher maturities (*4*, *24*, *26*). Bellincontro et al. (*31*) reported that inhibition of ethylene production in peach fruit affected volatile compound formation. This new data set from postharvest changes in aroma volatiles and ethylene production during peach fruit ripening provide a more comprehensive confirmation that the formation of aroma characteristics of peach is closely associated with ethylene biosynthesis. In apple fruit, Schaffer et al. (*14*) showed that fruit antisense for ACC oxidase produced no detectable ethylene and the fruit had very low aroma levels. External ethylene treatment could restore the ability of the fruit to develop an aroma characteristic of ripe fruit. Genes associated with the apple fruit aroma biosynthesis pathway also underwent ethylene regulation (*14*).

There was a similar set of gene expression patterns in the LOX family. There were similar trends with the declining expression of the two LOX genes *PpLOX2* and *PpLOX3* and the reduction in C6 compounds and, similarly, with the increase in *PpLOX1* and *PpLOX4* and lactone production in the late stage of senescence. Our previous study suggested a similar grouping of LOX genes in ripening kiwifruit (*35*). The major reduction in transcript levels of *PpLOX2* (more than 23-fold difference) and *PpLOX3* during the experimental period was similar to that of *AdLOX2*, *AdLOX3*, *AdLOX4*, and *AdLOX6* in ripening kiwifruit, although no particularly high similarities in sequence were found among these LOX genes in the two species. Ethylene-upregulated LOX gene

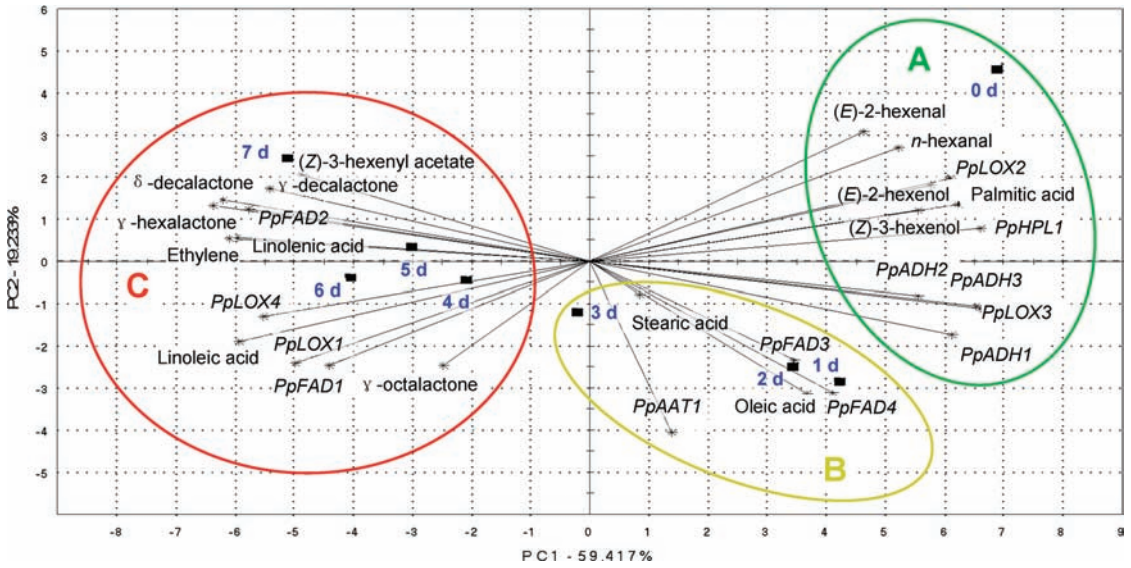

Figure 7. Plots of loading vectors of variables and the sample mean scores for the first two principal components of PCA for peach flesh ethylene, volatile compounds, and gene expression with postharvest ripening at 20 °C for 7 days. PC1 and PC2 accounted for 59.42 and 19.24% of the variation, respectively.

expression has also been found for tomato *TomLOXB* and *TomLOXC* (*39*), apple *MdLOX1* and *MdLOX7* (*14*), olive *Oep2LOX2* (*16*), and kiwifruit *AdLOX1* and *AdLOX5* (*36*). Chapman et al. (*32*) suggested that high levels of the C6 compounds in peach fruit were associated with LOX enzyme activity during fruit maturation. A particular role for LOX in plant volatile formation has arisen from transgenic work, when the removal of LOX resulted in a significant reduction in the levels of C6 compounds (*10*, *40*, *41*). It seems likely that the decline in green-note volatiles is due to a reduction of LOX gene expression (*15*).

LOX-mediated formation of fatty acid hydroperoxides can be quickly facilitated by the action of HPL. The expression of peach *PpHPL1* was relatively higher in fruit at harvest, where *n*-hexanal and (*E*)-2-hexenal were major contributors to peach fruit aroma. This is consistent with tomato fruit, where relatively high levels of *LeHPL1* mRNA were found in immature green fruit, whereas mature green and red fruit lacked detectable transcripts (*42*). The changes in HPL gene expression were related to the production of C6 aldehydes, which decreased during tomato fruit ripening (*10*). This developmentally regulated expression of HPL has also been reported in growing potato leaves and flowers (*43*). Antisense-mediated depletion of HPL in transgenic potato produced 1−3% the level of C6 compounds compared to that in nontransformed plants (*41*, *43*). However, transgenic *Arabidopsis*, in which HPL enzyme activity was enhanced to levels twice that in wild-type plants, did not cause significant changes in the C6 aldehyde (*Z*)-3-hexenal (*44*). From these results, it may be inferred that decreasing the expression of *PpHPL1* may be a factor contributing to the reduction in C6 aldehydes.

C6 hexanols, the other group of green-note volatiles, are produced by ADH using C6 aldehydes as substrates. A positive relationship between ADH activity and alcohol formation during peach fruit ripening has been reported (*31*). In the present study, downregulated expression in *PpADH1*, *PpADH2*, and *PpADH3* and decreased content in (*E*)-2-hexenol and (*Z*)-3-hexenol in postharvest ripening peach fruit were grouped together according to PCA, indicating an association between gene expression and generation of alcohols. A similar decreasing expression pattern has also been observed in apple fruit (*45*), and *MdADH1* has been suggested to be involved in volatile formation (*14*). Such changes in ADH transcripts contrast with observations in tomato (*46*), melon (*19*), and apricot (*20*) fruit, in which ADH genes were upregulated during fruit ripening. Recent studies reported that ADH contigs exhibited up- or downregulated expression during fruit ripening, such as peach (*47*) and nectarine (*48*). These results suggested that the regulation of ADH in ripening fruit may be independent of ethylene.

Alcohols can be used as substrates for the generation of esters by AAT, which is thought to be the last step in the LOX pathway. A rapid accumulation of AAT transcripts was observed during the first 2 days of postharvest ripening, which was the process that increased in esters. The present results showed that (*Z*)-3-hexenol tended to decline in peach fruit during postharvest ripening and is apparently used as a substrate for (*Z*)-3-hexenyl acetate formation. PCA showed that, with AAT gene expression, esters and alcohols were located in different groups, suggesting that either AAT or precursors alone were not especially important in ester biosynthesis. González-Agüero et al. (*20*) suggested that both AAT and alcohols were important factors for ester generation during apricot fruit ripening. The importance and function of AAT in fruit ester generation has been reported in apple (*21*), melon (*22*), and strawberry fruit (*23*). Our results showed significantly higher concentrations of esters and alcohol precursors in skin tissue when compared to that in the flesh of peach fruit; however, no significant difference in AAT gene expression was observed in different tissues (data not shown), indicating that substrates may play an important role in ester biosynthesis. In 'Rich Lady' peach fruit, it has been proposed that ester biosynthesis was limited in part by the supply of required substrate, suggesting that some critical steps for ester formation may be located upstream in the LOX pathway (*27*).

Fatty acids are precursors of volatile C6 compounds and lactones (*5*), and therefore, changes in fatty acid profiles and related gene expression were measured in ripening peach fruit. As previously reported (*49*), the present study showed that the predominant fatty acids were palmitic and linoleic acids in ripening fruit. After harvest, polyunsaturated fatty acids increased significantly, whereas the saturated fatty acids decreased, with the major changes occurring mostly between the climacteric and postclimacteric stages. PCA showed that linoleic and linolenic acids and *PpFAD1* and *PpFAD2* were located in one cluster, indicating a relationship between changes in fatty acids and expression of FAD genes. Blast searches showed that *PpFAD1*

had high identity (78% at the deduced amino acid sequence) to *Arabidopsis AtFAD2*, which is endoplasmic reticulum omega-6 desaturase and responsible for the formation of linoleic and linolenic acids (*50*). Mutant *fad2-1* plants had an increase in oleic acid and decrease in linoleic and linolenic acids (Germplasm/Stock: CS8041, www.arabidopsis.org). Peach *PpFAD2* was matched to *Arabidopsis AtFAD7* and *AtFAD8* (71 and 69% identities, respectively), which are chloroplast omega-3 desaturases and convert linoleic acid to linolenic acid (*50*). *Arabidopsis* mutant *fad7-1* and *fad8-1* exhibited a reduction in the desaturation of membrane lipids and an underproduction of linolenic acid (Germplasm/Stock: CS8036, www.arabidopsis.org).

In contrast with increasing linoleic and linolenic acid concentrations, levels of the C6 compounds were progressively reduced during peach fruit ripening and senescence. It seems unlikely that the decline in C6 aldehydes and alcohols is due to changes in fatty acid precursors during fruit ripening (*15*), although previous studies have shown that modification of fatty acid profiles can result in changes in volatile compounds (*7*, *8*). With regard to the synthesis of lactonic compounds, at least four pathways have been suggested and all lactones originate from fatty acids (*5*). As has been mentioned above, there was an inverse correlation between changes in saturated fatty acids and lactones during peach fruit ripening. PCA showed that increased linoleic and linolenic acids were grouped with upregulated lactones during ripening, indicating an association between changes in fatty acids and lactones. Epoxide hydrolase has been suggested to be involved in lactone biosynthesis through controlling the breakage of epoxide rings for the formation of two hydroxyl groups required for lactone cyclization, and genes encoding for the enzyme were mainly distributed in peach fruit skin tissue based on the results of comparative analysis of expressed sequence tags (*51*). Our results showed that concentrations of total lactones were 161.65 and 531.33 μg g^{-1} fresh weight (FW) at harvest time for flesh and skin tissue, respectively. They changed to 495.50 and 2277.25 μg g^{-1} FW after 7 days of ripening, respectively (data not shown). These results suggested that greater levels of epoxide hydrolase in the fruit skin tissue may be responsible for higher levels of lactones. The complete coding sequences of an epoxide hydrolase has been characterized from peach fruit and expressed in *Escherichia coli* to study the function of the enzyme (*51*).

The above findings taken together suggest that the fatty acid pathway plays an important role in determining the characteristic aroma profile during postharvest peach fruit ripening and senescence and is under regulation of ethylene. Ethylene upregulated *PpFAD1* and *PpFAD2* seem to be associated with the accumulation of linoleic and linolenic acids, which are used as precursors for LOX-mediated generation of aroma volatiles. Ethylene downregulated *PpLOX2*, *PpLOX3*, *PpHPL1*, *PpADH1*, *PpADH2*, and *PpADH3* were sensitive to ethylene-driven fruit ripening and may contribute to biosynthesis of grassy aroma aldehydes and alcohols. The generation of characteristic lactones paralleled the climacteric rise in ethylene production and seems to be related to changes in fatty acid components in ripening fruit. Grassy-note aldehydes and alcohols initially derived from the fatty acid pathway are replaced by fruity-note lactones as the aroma profile changes with peach fruit ripening. Although these relationships between levels of aroma compounds, gene expression, and peach fruit ripening are correlative, the patterns are logical but need confirmation through more analysis. With the release of new sequences generated from peach EST projects and whole genome sequencing, more gene family members may be found in the near future and a more comprehensive study of all available genes will be needed to determine roles and mechanisms for volatile production in fruit, such as a peach.

LITERATURE CITED

(1) Aubert, C.; Milhet, C. Distribution of the volatile compounds in the different parts of a white-fleshed peach (*Prunus persica* L. Batsch). *Food Chem.* **2007**, *102*, 375–384.

(2) Wang, Y. J.; Yang, C. X.; Li, S. H.; Yang, L.; Wang, Y. N.; Zhao, J. B.; Jiang, Q. Volatile characteristics of 50 peaches and nectarines evaluated by HP-SPME with GC−MS. *Food Chem.* **2009**, *116*, 356–364.

(3) Horvat, R. J.; Chapman, G. W.; Robertson, J. A.; Meredith, F. I.; Scorza, R.; Callahan, A. M.; Morgens, P. Comparison of the volatile compounds from several commercial peach cultivars. *J. Agric. Food Chem.* **1990**, *38*, 234–237.

(4) Kakiuchi, N.; Ohmiya, A. Changes in the composition and content of volatile constituents in peach fruits in relation to maturity at harvest and artificial ripening. *J. Jpn. Soc. Hortic. Sci.* **1991**, *60*, 209–216.

(5) Schwab, W.; Davidovich-Rikanati, R.; Lewinsohn, E. Biosynthesis of plant-derived flavor compounds. *Plant J.* **2008**, *54*, 712–732.

(6) Dudareva, N.; Pichersky, E. Metabolic engineering of plant volatiles. *Curr. Opin. Biotechnol.* **2008**, *19*, 181–189.

(7) Cañoles, M. A.; Beaudry, R. M. Deficiency of linolenic acid in Lefad7 mutant tomato changes the volatile profile and sensory perception of disrupted leaf and fruit tissue. *J. Am. Soc. Hortic. Sci.* **2006**, *131*, 284–289.

(8) Wang, C. L.; Chin, C. K.; Ho, C. T.; Hwang, C. F.; Polashock, J. J.; Martin, C. E. Changes of fatty acids and fatty acid-derived flavor compounds by expression the yeast Δ-9 desaturase gene in tomato. *J. Agric. Food Chem.* **1996**, *44*, 3399–3402.

(9) Wang, C. L.; Xing, J. S.; Chin, C. K.; Ho, C. T.; Martin, C. E. Modification of fatty acids changes the flavor volatiles in tomato leaves. *Phytochemistry* **2001**, *58*, 227–232.

(10) Chen, G. P.; Hackett, R.; Walker, D.; Taylor, A.; Lin, Z. F.; Grierson, D. Identification of a specific isoform of tomato lipoxygenase (TomloxC) involved in the generation of fatty acid-derived flavor compounds. *Plant Physiol.* **2004**, *136*, 2641–2651.

(11) Matsui, K.; Fukutomi, S.; Wilkinson, J.; Hiatt, B.; Knauf, V.; Kajwara, T. Effect of overexpression of fatty acid 9-hydroperoxide lyase in tomatoes (*Lycopersicon esculentum* Mill.). *J. Agric. Food Chem.* **2001**, *49*, 5418–5424.

(12) Speirs, J.; Lee, E.; Holt, K.; Yong-Duk, K.; Scott, N. S.; Loveys, B.; Schuch, W. Genetic manipulation of alcohol dehydrogenase levels in ripening tomato fruit affects the balance of some flavor aldehydes and alcohols. *Plant Physiol.* **1998**, *117*, 1047–1058.

(13) Defilippi, B. G.; Manríquez, D.; Luengwilai, K.; González-Agüero, M. Aroma volatiles: Biosynthesis and mechanisms of modulation during fruit ripening. In *Advances in Botanical Research*; Kader, J. C., Delseny, M., Eds.; Academic Press: New York, 2009; Vol. 50, pp 1−37.

(14) Schaffer, R. J.; Friel, E. N.; Souleyre, E. J. F.; Bolitho, K.; Thodey, K.; Ledger, S.; Bowen, J. H.; Ma, J. H.; Nain, B.; Cohen, D.; Gleave, A. P.; Crowhurst, R. N.; Janssen, B. J.; Yao, J. L.; Newcomb, R. D. A genomics approach reveals that aroma production in apple is controlled by ethylene predominantly at the final step in each biosynthetic pathway. *Plant Physiol.* **2007**, *144*, 1899–1912.

(15) Zhang, B.; Yin, X. R.; Li, X.; Yang, S. L.; Ferguson, I.; Chen, K. S. Lipoxygenase gene expression in ripening kiwifruit in relation to ethylene and aroma production. *J. Agric. Food Chem.* **2009**, *57*, 2875–2881.

(16) Padilla, M. N.; Hernández, M. L.; Sanz, C.; Martínez-Rivas, J. M. Functional characterization of two 13-lipoxygenase genes from olive fruit in relation to the biosynthesis of volatile compounds of virgin olive oil. *J. Agric. Food Chem.* **2009**, *57*, 9097–9107.

(17) Tijet, N.; Wäspi, U.; Gaskin, D. J. H.; Hunziker, P.; Muller, B. L.; Vulfson, E. N.; Slusarenko, A.; Brash, A. R.; Whitehead, I. M. Purification, molecular cloning, and expression of the gene encoding fatty acid 13-hydroperoxide lyase from guava fruit (*Psidium guajava*). *Lipids* **2000**, *35*, 709–720.

(18) Tijet, N.; Schneider, C.; Muller, B. L.; Brash, A. R. Biogenesis of volatile aldehydes from fatty acid hydroperoxides: Molecular cloning of a hydroperoxide lyase (CYP74C) with specificity for both the 9- and 13-hydroperoxides of linoleic and linolenic acids. *Arch. Biochem. Biophys.* **2001**, *386*, 281–289.

(19) Manríquez, D.; Ei-Sharkawy, I.; Flores, F. B.; Ei-Yahyaoui, F.; Regad, F.; Bouzayen, M.; Latché, A.; Pech, J. C. Two highly divergent alcohol dehydrogenases of melon exhibit fruit ripening-specific expression and distinct biochemical characteristics. *Plant Mol. Biol.* **2006**, *61*, 675–685.
(20) González-Agüero, M.; Troncoso, S.; Gudenschwager, O.; Gampos-Vargas, R.; Moya-León, M. A.; Defilippi, B. G. Differential expression levels of aroma-related genes during ripening of apricot (*Prunus armeniaca* L.). *Plant Physiol. Biochem.* **2009**, *47*, 435–440.
(21) Zhu, Y.; Rudell, D. R.; Mattheis, J. P. Characterization of cultivar differences in alcohol acyltransferase and 1-aminocyclopropane-1-carbooxylate synthase gene expression and volatile ester emission during apple fruit maturation and ripening. *Postharvest Biol. Technol.* **2008**, *49*, 330–339.
(22) Ei-Sharkawy, I.; Manrríquez, D.; Flores, F. B.; Regad, F.; Bouzayen, M.; Latché, A.; Pech, J. C. Functional characterization of a melon alcohol acyl-transferase gene family involved in the biosynthesis of ester volatiles. Identification of the crucial role of a threonine residue for enzyme activity. *Plant Mol. Biol.* **2005**, *59*, 345–362.
(23) Aharoni, A.; Keizer, L. C. P.; Bouwmeester, H. J.; Sun, Z.; Alvarez-Huerta, M.; Verhoeven, H. A.; Blaas, J.; van Houwelingen, A. M. M. L.; De Vos, R. C. H.; van der Voet, H.; Jansen, R. C.; Guis, M.; Mol, J.; Davis, R. W.; Schena, M.; van Tunen, A. J.; O'Conell, A. P. Identification of the SAAT gene involved in strawberry flavor biogenesis by use of DNA microarrays. *Plant Cell* **2000**, *12*, 647–661.
(24) Horvat, R. J.; Chapman, G. W. Comparison of volatile compounds from peach fruit and leaves during maturation. *J. Agric. Food Chem.* **1990**, *38*, 1442–1444.
(25) Lavilla, T.; Recasens, I.; Lopez, M. L.; Puy, J. Multivariate analysis of maturity stages, including quality and aroma, in 'Royal Glory' peaches and 'Big Top' nectarines. *J. Sci. Food Agric.* **2002**, *82*, 1842–1849.
(26) Visai, C.; Vanoli, M. Volatile compound production during growth and ripening of peaches and nectarines. *Sci. Hortic.* **1997**, *70*, 15–24.
(27) Ortiz, A.; Echeverría, G.; Graell, J.; Lara, I. Overall quality of 'Rich Lady' peach fruit after air- or CA storage. The importance of volatile emission. *LWT—Food Sci. Technol.* **2009**, *42*, 1520–1529.
(28) Raffo, A.; Nardo, N.; Tabilio, M. R.; Paoletti, F. Effects of cold storage on aroma compounds of white- and yellow-fleshed peaches. *Eur. Food Res. Technol.* **2008**, *226*, 1503–1512.
(29) Robertson, J. A.; Meredith, F. I.; Horvat, R. J.; Senter, S. D. Effect of cold storage and maturity on the physical and chemical characteristics and volatile constituents of peaches (cv. Cresthaven). *J. Agric. Food Chem.* **1990**, *38*, 620–624.
(30) Yang, D. S.; Balandrán-Quintana, R. R.; Ruiz, C. F.; Toledo, R. T.; Kays, S. J. Effect of hyperbaric, controlled atmosphere, and UV treatments on peach volatiles. *Postharvest Biol. Technol.* **2009**, *51*, 334–341.
(31) Bellincontro, A.; Morganti, F.; DeSantis, D.; Botondi, R.; Mencarelli, F. Inhibition of ethylene via different ways affects LOX and ADH activities, and related volatiles compounds in peach (cv. 'Royal Gem'). *Acta Hortic.* **2005**, *682*, 445–452.
(32) Chapman, G. W.; Horvat, R. J.; Forbus, W. R. Physical and chemical changes during the maturation of peaches (cv. Majestic). *J. Agric. Food Chem.* **1991**, *39*, 867–870.
(33) Infante, R.; Farcuh, M.; Meneses, C. Monitoring the sensorial quality and aroma through an electronic nose in peaches during cold storage. *J. Sci. Food Agric.* **2008**, *88*, 2073–2078.
(34) Infante, R.; Meneses, C.; Rubio, P.; Seibert, E. Quantitative determination of flesh mealiness in peach [*Prunus persica* L. (Batch.)] through paper absorption of free juice. *Postharvest Biol. Technol.* **2009**, *51*, 118–121.
(35) Zhang, B.; Chen, K. S.; Bowen, J.; Allen, A.; Espley, R.; Karunairetnam, S.; Ferguson, I. Differential expression within the LOX gene family in ripening kiwifruit. *J. Exp. Bot.* **2006**, *57*, 3825–3836.
(36) Lazzari, B.; Caprera, A.; Vecchietti, A.; Stella, A.; Milanesi, L.; Pozzi, C. ESTree db: A tool for peach functional genomics. *BMC Bioinf.* **2005**, *6*, S16.
(37) Tong, Z. G.; Gao, Z. H.; Wang, F.; Zhou, J.; Zhang, Z. Selection of reliable reference genes for gene expression studies in peach using real-time PCR. *BMC Mol. Biol.* **2009**, *10*, 71.
(38) Zhang, B.; Yin, X. R.; Shen, J. Y.; Ferguson, I. B.; Chen, K. S. Volatiles production and lipoxygenase gene expression in kiwifruit peel and flesh at two ripening stages. *J. Am. Soc. Hortic. Sci.* **2009**, *134*, 472–477.
(39) Griffiths, A.; Barry, C.; Alpuche-Solis, A. G.; Grierson, D. Ethylene and developmental signals regulate expression of lipoxygenase genes during tomato fruit ripening. *J. Exp. Bot.* **1999**, *50*, 793–798.
(40) León, J.; Royo, J.; Vancanneyt, G.; Sanz, C.; Silkowaski, H.; Griffiths, G.; Sánchez-Serrano, J. J. Lipoxygenase H1 gene silencing reveals a specific role in supplying fatty acid hydroperoxides for aliphatic aldehyde production. *J. Biol. Chem.* **2002**, *277*, 416–423.
(41) Salas, J. J.; Sánchez, C.; García-González, D. L.; Aparicio, R. Impact of the suppression of lipoxygenase and hydroperoxide lyase on the quality of the green odor in green leaves. *J. Agric. Food Chem.* **2005**, *53*, 1648–1655.
(42) Howe, G. A.; Lee, G. I.; Itoh, A.; Li, L.; DeRocher, A. E. Cytochrome P450-dependent metabolism of oxylipins in tomato. Cloning and expression of allene oxide synthase and fatty acid hydroperoxide lyase. *Plant Physiol.* **2000**, *123*, 711–724.
(43) Vancanneyt, G.; Sanz, C.; Farmaki, T.; Paneque, M.; Ortego, F.; Castañera, P.; Sánchez-Serrano, J. J. Hydroperoxide lyase depletion in transgenic potato plants leads to an increase in aphid performance. *Proc. Natl. Acad. Sci. U.S.A.* **2001**, *98*, 8139–8144.
(44) Shiojiri, K.; Kishimoto, K.; Ozawa, R.; Kugimiya, S.; Urashimo, S.; Arimura, G.; Horiuchi, J.; Nishioka, T.; Matsui, K.; Takabayashi, J. Changing green leaf volatile biosynthesis in plants: An approach for improving plant resistance against both herbivores and pathogens. *Proc. Natl. Acad. Sci. U.S.A.* **2006**, *103*, 16672–16676.
(45) Defilippi, B. G.; Kader, A. A.; Dandekar, A. M. Apple aroma: Alcohol acyltransferase, a rate limiting step for ester biosynthesis, is regulated by ethylene. *Plant Sci.* **2005**, *168*, 1199–1210.
(46) Longhurst, T.; Lee, E.; Hinde, R.; Brady, C.; Speirs, J. Structure of the tomato *Adh2* gene and *Adh2* pseudogenes, and a study of *Adh2* gene expression in fruit. *Plant Mol. Biol.* **1994**, *26*, 1073–1084.
(47) Trainotti, L.; Tradiello, A.; Casadoro, G. The involvement of auxin in the ripening of climacteric fruits comes of age: The hormone plays a role of its own and has an intense interplay with ethylene in ripening peaches. *J. Exp. Bot.* **2007**, *58*, 3299–3308.
(48) Ziliotto, F.; Begheldo, M.; Rasori, A.; Bonghi, C.; Tonutti, P. Transcriptome profiling of ripening nectarine (*Prunus persica* L. Batsch) fruit treated with 1-MCP. *J. Exp. Bot.* **2008**, *59*, 2781–2791.
(49) Izzo., R.; Scartazza, A.; Masia, A.; Galleschi, L.; Quartacci, M. F.; Navari-Izzo, F. Lipid evolution during development and ripening of peach fruits. *Phytochemistry* **1995**, *39*, 1329–1334.
(50) Maeda, H.; Sage, T. L.; Isaac, G.; Welti, R.; DellaPenna, D. Tocopherols modulate extraplastidic polyunsaturated fatty acid metabolism in *Arabidopsis* at low temperature. *Plant Cell* **2008**, *20*, 452–470.
(51) Vecchietti, A.; Lazzari, B.; Ortugno, C.; Bianchi, F.; Malinverni, R.; Caprera, A.; Mignani, I.; Pozzi, C. Comparative analysis of expressed sequence tags from tissues in ripening stages of peach (*Prunus persica* L. Batsch). *Tree Genet. Genomes* **2009**, *5*, 377–391.

Received for review January 15, 2010. Revised manuscript received April 9, 2010. Accepted April 15, 2010. This research was supported by the National Natural Science Foundation of China (30771495 and 30800739), the National Project of Scientific and Technical Supporting Programs funded by the Ministry of Science and Technology of China (2006BAD22B05), the Special Scientific Research Fund of the Agricultural Public Welfare Profession of China (200903044), the Science and Technology Project of Zhejiang Province (2007C12069), the Ningbo Science and Technology Project (2006C100029), the Science Foundation of Chinese University, the 111 Project (B06014), and Zhejiang University K. P. Chao's Hi-Tech Foundation for Scholars and Scientists.